



Electromagnetism-Enabled Transmitter of Molecular Communications Using Ca^{2+} Signals

Peng He^{1,2,3(✉)} and Donglai Tang⁴

¹ School of Communication and Information Engineering, Chongqing University of Posts and Telecommunications, Chongqing, China

² Key Laboratory of Optical Communication and Networks in Chongqing, Chongqing, China

³ Key Laboratory of Ubiquitous Sensing and Networking in Chongqing, Chongqing, China

⁴ Aostar Information Technologies Co., Ltd., Beijing, China
tangdonglai@sgitg.sgcc.com.cn

Abstract. Molecular Communications provides a promising solution to achieve precise control and process of bio-things in applications of Healthcare-IoT. In this paper, we investigate the mechanism of electromagnetism-induced molecular communications (EMC) among non-excitabile biological cell networks. We choose calcium signals as the physical information carrier to study the paradigm of EMC. Firstly, an electromagnetism-potential coupling model is established to study the electric-magnetic induction behaviour of cellular membrane potential. Then, an Ca^{2+} oscillation model is established to study the relation between membrane potential and Ca^{2+} signals. Further, we validate the waveform patterning of calcium signaling by applying various intensities and frequencies of electromagnetism. This paper shows the relations between electromagnetism stimuli and calcium oscillation through mathematical modeling and numerical experiments. We find that there exists a resonance behavior between electromagnetism and calcium signals, namely calcium signals oscillate via a similar frequency with the electromagnetism. This paper reveals that molecular communication can be effectively induced by traditional electromagnetic signals.

Keywords: Molecular communications · Electromagnetism-enabled · Calcium signals · Transmitter design

Supported by the National Natural Science Foundation of China (Grant No. 61901070, 61871062, 61771082, 61801065), partially supported by the Science and Technology Research Program of Chongqing Municipal Education Commission (Grant No. KJQN201900611, KJQN201900604), and partially supported by Program for Innovation Team Building at Institutions of Higher Education in Chongqing (Grant No. CXTDX201601020).

1 Introduction

Progress of precise healthcare applications requires nano-scale process technologies of bio-things in intra-body environment, where most traditional IoT devices are not tiny and bio-compatible enough for intra-body applications [1]. Molecular communications (MC) are proposed as a new communication paradigms which enables multiple of nano-machines to cooperate for various nano-scale tasks [2]. In a MC system, nano-machines act as different roles including transceiver and relays to process information of nano-scale networks.

In this work, we choose Ca^{2+} signals as the information carrier for MC communication system due to follow two considerations. First, Ca^{2+} signals is one of the most important physiological signals in vivo. Ca^{2+} signals is the well-known second messenger, which plays critical roles in many metabolism processes and is closely associated with many diseases. Thereby Ca^{2+} signals are worthy to be investigated in the research scope of biology and medicines. Second, Ca^{2+} signals appear as some patterns of waveforms, that is similar to the electromagnetic wave. In the ideal environment, Ca^{2+} signals even propagate as the periodic waves of impulses, the amplitudes and frequency of impulses can be regulated via some bio-engineering methods.

A simplest MC system can be divided into a transmitter, a receiver and the communication channel according to the physical layer concept. Plenty of literatures have addressed on the work of receiver technologies, which aims to extract the information from the absorbed molecules around the receivers. Typical cases are like signal detection [3], decoding or demodulation [4], ISI-elimination [5], etc. Research on MC channel enables nano-machines adapts the unique characters of the special channels. Typical cases are channel coding [6], channel modelling [7], channel synchronization [8], etc. Transmitter is another important unit in communication system. However, limited literatures try to study MC from the aspect of transmitter. In [9], a multiple transmitter local drug delivery system associated with encapsulated drug transmitters was investigated. In [10], the authors discussed issues concerned with transmission rate control in molecular communication, an emerging communication paradigm for bio-nanomachines in an aqueous environment. In [11], the authors modeled the molecule emission process more accurately using rectangular and exponential transmit signals and derived closed form expressions for the number of molecules that are absorbed by the receiver in a diffusion-Based MC system.

To design the transmitter, an unsolved challenge is how to trigger and control nano-machines directly in bio-systems. Embedded nano-machines placed in various organs, tissues and cells, which need programmable instructions. One major class of existing solutions are enabling nano-machine with intelligent abilities via some bio-engineering methods. For example, DNA robots equipped with recombinant nucleotides are capable of storing, moving and reacting in the biological networks [12]. Bacteria can also be modified using filled nucleotides to express various functions of nano-machines. Another way to trigger biological signals can be from external space. Plenty of experiment results reveal that some physical

or chemical stimuli can effectively induce various biological signals and promote metabolism of bio-systems [13].

In this work, we consider a non-excitabile epidermis cell as the transmitter in MC system. We propose a controllable designed transmitter for MC system. With the inspiration of external electromagnetism, the transmitter cell is able to generate various patterns of waveforms in the communication process in the design. By adjusting the parameters of electromagnetism, we can adjust the amplitude and frequency of the waveforms, in order to express the various bits in the coding. We establish a model of Ca^{2+} signal generation, which is divided into electromagnetism-potential coupling phase and Potential-induced Ca^{2+} signal phase. In the first phase, the electromagnetism act on the cell membrane and elevate the its potential. In the second phase, the elevated membrane potential promote the release of Ca^{2+} ions from organelles to generate MC signals.

The rest of this paper is organized as follows. Section 2 introduces the transmitter design of MC. Section 3 shows numerical results to demonstrate the capability and performance of the designed transmitters. Section 4 gives a summary of this work to conclude the paper.

2 System Overview

The proposed MC system is presented in Fig. 1, which is composed of an electromagnetic device and biological epidermis cells belonging to human-beings. We assume that the electromagnetic device is regarded as the controller, which is capable to actuate the transmitter by emitting low-frequency electromagnetic waves. The low-frequency electromagnetic waves are regarded as the controlling massages, which effects on biological cells and lead a series of bio-chemical reactions epidermis cells. We choose sine save to contain the controlling massages due to its univarsity in application of wireless communications. Epidermis cells are regarded as the transmitter, where Ca^{2+} concentration of epidermis cells oscillate as various patterns of waveforms to trigger MC process. In this work, we focus on the transmitter design in one single cell, namely, we ignore the interactions between different connected cells.

3 Electromagnetism-Enabled Transmitter Design

The proposed transmitter includes two phases, which are electromagnetism-potential coupling phase and potential-induced Ca^{2+} signaling phase.

3.1 Electromagnetism-Potential Coupling Phase

Let $I = E_m \sin(2\pi ft)$ denotes the alternating electromagnetism as the system input with electromagnetism intensity E_m and alternating frequency f . The potential of the cell membrane is raised due the movement of electric ions, which is promoted by three different classes of forces, expressed by,

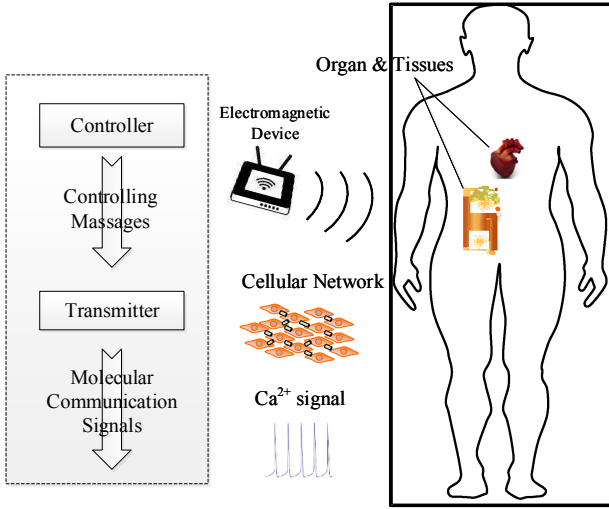


Fig. 1. Proposed system model

$$m \frac{d^2l}{dt^2} - F_3 + F_1 = F_2 \tag{1}$$

where l is the moving distance of electric ion compared to the initial position during the moving process.

The first class of force is restoring force resulted by electrochemical gradient,

$$F_1 = -m\omega^2l \tag{2}$$

where m is the quality of the electric ion, and $\omega = 2\pi f_s$ is the self-sustained oscillation angular frequency. Accordingly, f_s is the self-sustained oscillation frequency.

The second class of force is the external force brought by the electromagnetism, expressed by,

$$F_2 = E_m z q_e \sin(2\pi f t) \tag{3}$$

where z is the valence state of the electric ion. $q_e = 1.6 * 10^{-19}$ C is the unit electric charge.

The third class of force is decaying force, expressed by,

$$F_3 = -\lambda \frac{dl}{dt} \tag{4}$$

where λ is the attenuation coefficient. The approximated solution of Eq. (1) is given by,

$$l = -\frac{E_m z q_e}{2\pi \lambda v} \cos(2\pi v t) \tag{5}$$

In this work, we consider the effect of electromagnetism on SOC channel on the cellular membrane, resulted by a force [],

$$F = \frac{1}{4\pi\epsilon\epsilon_0} \cdot \frac{q \cdot zq_e}{r^2} \quad (6)$$

where ϵ_0 is the vacuum dielectric constant, ϵ is the relative dielectric constant, $q = 1.6 * q_e$ is the charge of SOC channel. r is the distance between the free charge and SOC channel. Cellular membrane potential is related to the membrane thickness s , the effect force F and the charge q , expressed by,

$$V_m = F \cdot \frac{s}{q} \quad (7)$$

Through a differential operation, we have,

$$\partial V_m = \partial F \cdot \frac{s}{q} \quad (8)$$

Take the expression of Eq. (6) into (8), we have,

$$\partial V_m = \frac{1}{2\pi\epsilon\epsilon_0} \cdot \frac{q \cdot zq_e}{r^3} \partial r \quad (9)$$

Assume that position of the electrical ion is the origin, then $\partial x = \partial r$ holds. By integrating Eq. (5) and (8) into (9), the variation of membrane potential is give by,

$$\partial V_m = \frac{1}{2\pi\epsilon\epsilon_0} \cdot \frac{q \cdot zq_e}{r^3} \cdot \frac{s}{q} \cdot \frac{E_0 zq_e}{\lambda} \sin(2\pi vt) \partial t \quad (10)$$

3.2 Potential-Induced Ca²⁺ Signaling Phase

A widely-accepted model [16] of calcium dynamic is adopted to describe the intracellular oscillation process, which is shown in Fig. 2. For cell i in the network, two variables x_i and y_i are respectively used to describe the Ca²⁺ concentrations in the cytoplasm and internal store. The Ca²⁺ dynamics is described by the set of equations below.

$$\frac{dx}{dt} = P_1 - P_2 + P_3 + a_1 y - a_2 x + I_G, \quad (11)$$

$$\frac{dy}{dt} = P_2 - P_3 - a_1 y, \quad (12)$$

where

$$Q_1 = b_1 + b_2(t) \quad (13)$$

$$P_2 = \frac{b_3 \cdot x^2}{b_4^2 + x^2}, \quad (14)$$

$$P_3 = \frac{b_5 \cdot x^4 y^4}{(b_6^4 + x^4)(b_7^2 + y^4)}. \quad (15)$$

P_1 denotes the Ca^{2+} increase from the extracellular space via different classes of channels. P_2 and P_3 determine the Ca^{2+} exchange between the cytoplasm and internal stores due to the regulation of channel permeability. In P_1 , b_1 denotes non-electromagnetism-induced Ca^{2+} increase due to the constant pumping of Ca^{2+} influx. $b_2(t)$ denotes Ca^{2+} increase due to the promotion of electromagnetism. In this model, the expression of $b_2(t)$ is related with change of membrane potential V_m ,

$$C_m \frac{dV_m}{dt} = b_2(t) \quad (16)$$

where C_m is the capacitance of the cell membrane.

4 Performance Evaluation

In this section, we present the patterning behaviours of Ca^{2+} signals induced by the transmitter. The target of the simulation is to validate the availability and performance of the proposed transmitter.

4.1 Simulation Configuration

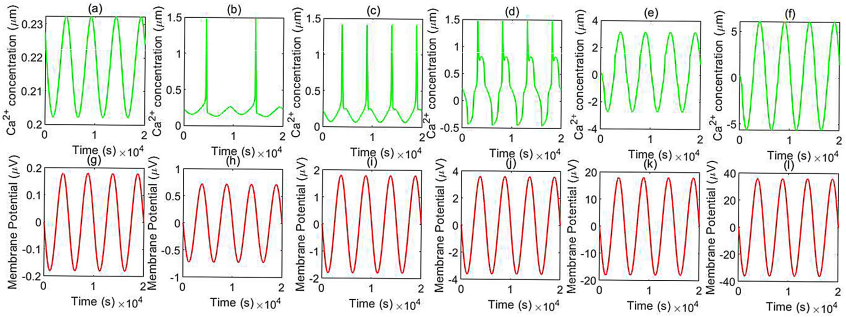
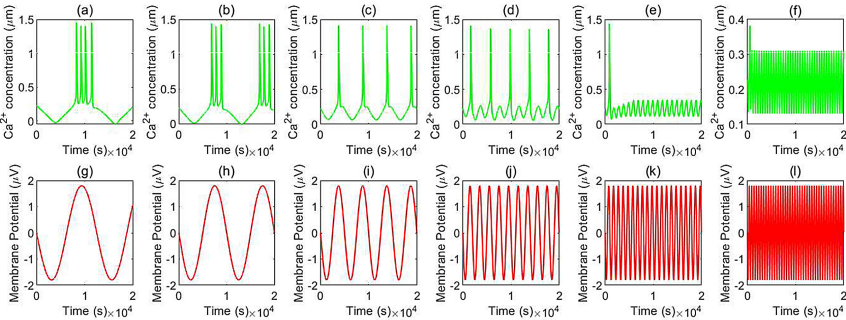
The parameter configures include two parts: the first part is parameters of electromagnetism-potential coupling phase, which is listed in Table 1 [14,15]; the second part is parameters of potential-induced Ca^{2+} signaling phase, listed in Table 2 [16,17].

Table 1. Electromagnetism-potential coupling parameters

Parameter	Value
q_e	10^{-19} C
q	$1.7 * q_e$ C
z	1
ε	4
ε_0	$8.854 * 10^{-12}$ $\text{N}^{-1} \text{m}^{-2} \text{C}^2$
r	10^{-9} m
s	10^{-8} m
λ	$6.4 * 10^{-12}$ kg/s

Table 2. Ca^{2+} signaling parameters

Parameter	Value
a_1	1 s^{-1}
a_2	6 s^{-1}
b_1	$1.3 \text{ } \mu\text{ms}^{-1}$
b_3	$65 \text{ } \mu\text{ms}^{-1}$
b_4	$1 \text{ } \mu\text{m}$
b_5	$500 \text{ } \mu\text{ms}^{-1}$
b_6	$0.9 \text{ } \mu\text{m}$
b_7	$2.0 \text{ } \mu\text{m}$

**Fig. 2.** Waveform patternings of membrane potential (V_m) and Ca^{2+} signals (x) under different E_m , $f = 0.2 \text{ Hz}$, (a) (g) $E_m = 0.0005 \text{ mV/m}$, (b) (h) $E_m = 0.002 \text{ mV/m}$, (c) (i) $E_m = 0.005 \text{ mV/m}$, (d) (j) $E_m = 0.01 \text{ mV/m}$, (e) (k) $E_m = 0.05 \text{ mV/m}$, (f) (l) $E_m = 0.01 \text{ mV/m}$.**Fig. 3.** Waveform patternings of membrane potential (V_m) and Ca^{2+} signals (x) under different f , $E_m = 0.005 \text{ mV/m}$, (a) (g) $f = 0.08 \text{ Hz}$, (b) (h) $f = 0.1 \text{ Hz}$, (c) (i) $f = 0.2 \text{ Hz}$, (d) (j) $f = 0.5 \text{ Hz}$, (e) (k) $f = 1 \text{ Hz}$, (f) (l) $f = 2 \text{ Hz}$.

4.2 Waveform Patterning Presentation

In Fig. 2, we check the waveform patterning of membrane potential and Ca^{2+} signaling by regulating E_m . Curves of (a) to (f) denote the waveforms of Ca^{2+} concentration (i.e., x), and curves of (g) to (i) denote the membrane potential (i.e., V_m). We can see that V_m changes as a sine shape, that is also presented in Eq. (10). Increase of E_m amplifies the amplitude of V_m from 0.2 to 40 μV , while its oscillation frequency keep the same with f (4 periods in 20 s). By observing the Ca^{2+} concentration x , we see that x performs as sine wave when E_m is small ($E_m = 0.0005 \text{ mV/m}$), then becomes the impulse arrays when E_m is a little larger ($E_m = 0.002, 0.005 \text{ mV/m}$), and becomes approximated sine waveforms when E_m is large enough $E_m = 0.01, 0.05, 0.1 \text{ mV/m}$. According to existing knowledge, Ca^{2+} signals perform as impulse arrays when cells function normally. So we have the following findings: 1) Ca^{2+} signals perform as normal impulse arrays just when E_m locates in a suitable area; 2) High intensities of E_m break the normal impulse patterning of Ca^{2+} signals and turn it into sine waves.

Similarly, we check the waveform patterning of membrane potential and Ca^{2+} signals by regulating their frequencies f in Fig. 3. Curves of (a) to (f) denote the waveforms of Ca^{2+} concentration (i.e., x), and curves of (g) to (i) denote the membrane potential (i.e., V_m). In this figure, V_m changes as a sine shape, and its frequency increases under different f . When f is small, one E_m peak evoke different number of Ca^{2+} impulses. The impulse number per V_m peak is initially 4 when $f = 0.08 \text{ Hz}$, decrease into 3 when $f = 0.1 \text{ Hz}$, and finally becomes 1 when $f = 0.2 \text{ Hz}$. Ca^{2+} impulses change and then disappear when f is regulated from 0.5 to 1 Hz. When $f = 2 \text{ Hz}$, Ca^{2+} seems to perform as dense sine waveforms. We find that slow oscillation of electromagnetism evoke discrete Ca^{2+} impulses, and fast oscillation of electromagnetism turn Ca^{2+} signals into sine waves.

4.3 Waveform Similarity Analysis

Based on the similarity of curves in Fig. 2 and 3, we apply a signal correlation coefficient (denoted by ρ) to quantify the waveform similarity between Ca^{2+} signals and membrane potential signals. ρ is given by,

$$\rho = \frac{E((x - E(x))(V_m - E(V_m)))}{\sqrt{E((x - E(x))^2)E((V_m - E(V_m))^2)}} \quad (17)$$

where $E(\cdot)$ is the average function. Obviously, ρ locates in area of $[-1, 1]$;

In Fig. 4, we validate the relationship between the signal correlation coefficient ρ and electromagnetism intensity E_m under different f . It can be seen that with the increase of E_m , ρ firstly drop quickly from 0.9 during a small change of E_m , and then rise slowly until recover to steady level. There exists a minimum point for ρ by altering E_m . Also, various f make difference for ρ . when $f = 0.1 \text{ Hz}$, ρ could reach to nearly 1 if E_m is 0.02 mV/m , while ρ could just reach to nearly 0.7 when $f = 1 \text{ Hz}$. The minimum point of ρ also increases with increase of f .

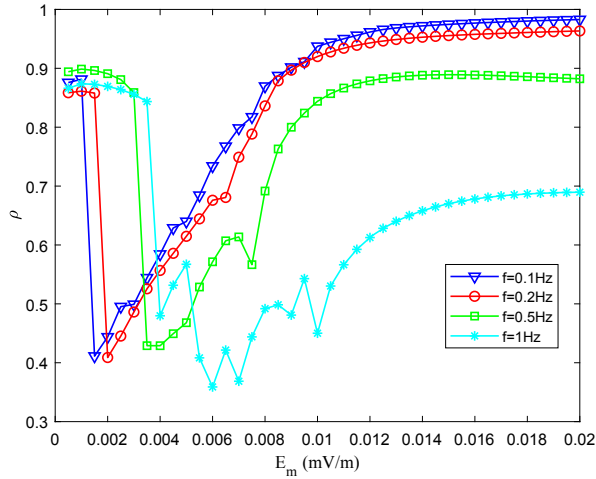


Fig. 4. Signal correlation coefficient ρ with variation of E_m under different f .

In Fig. 5, we validate the relationship between the Signal correlation coefficient ρ with variation of f under different E_m . It can be seen that with the increase of f , ρ firstly drops and then rise. There exists a minimum point for ρ by altering f . Also, various E_m make difference for ρ . when $E_m = 0.0005$ mV/m, the minimum point is around from 0.4 to 0.6, and the rise of ρ is very slow around 0. when $E_m = 0.005$ mV/m, the minimum point of f is located in 1.4 Hz, and ρ rise quickly then fall again. Similar case holds when $E_m = 0.008$ mV/m,

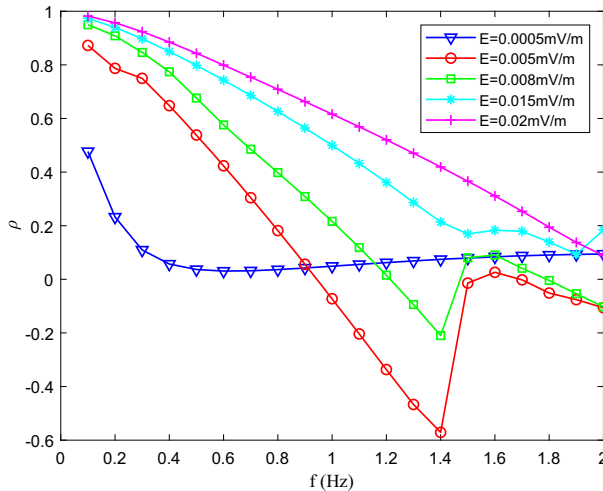


Fig. 5. Signal correlation coefficient ρ with variation of f under different E_m .

their minimum points are quite close. When $E_m = 0.015$ mV/m, the minimum point moves to around 1.8 Hz.

To precisely control the transmitter, we wish to avoid the minimal point and increase ρ . Above two figures tell us that there are some bad performance cases when we alter the value of E_m and f . The trends of the curves guide us to increase the communication performance and controllability of the transmitter.

5 Conclusion

In this paper, we investigated the issue of electromagnetism-enabled transmitter design for molecular communications. We proposed a MC framework which utilize electromagnetism waves to actuate the transmitter. In the transmitter design, an electromagnetism-potential coupling model is proposed to establish a bridge between electromagnetism signals and biological signals. We further extend the oscillation models of Ca^{2+} by integrating the variation of membrane potential.

This paper shows that electromagnetism-enabled transmitter of molecular communications are feasible through mathematical modeling and numerical results. Future work includes the extension of proposed method from single cell to multiple cells, and experiment validation of electromagnetism-induced molecular communications.

References

1. Akyildiz, I.F., Brunetti, F., Blazquez, C.: Nanonetworks: a new communication paradigm. *Comput. Netw.* **52**(12), 2260–2279 (2008)
2. Farsad, N., Yilmaz, H.B., Eckford, A., Chae, C., Guo, W.: A comprehensive survey of recent advancements in molecular communication. *IEEE Commun. Surv. Tutor.* **18**(3), 1887–1919 (2016). <https://doi.org/10.1109/COMST.2016.2527741>
3. Aslan, E., Pekergin, F., Çelebi, M.E.: Receiver detection methods on molecular communications. In: 2020 28th Signal Processing and Communications Applications Conference (SIU), pp. 1–4 (2020). <https://doi.org/10.1109/SIU49456.2020.9302509>
4. Chou, C.T.: Maximum a-posteriori decoding for diffusion-based molecular communication using analog filters. *IEEE Trans. Nanotechnol.* **14**(6), 1054–1067 (2015). <https://doi.org/10.1109/TNANO.2015.2469301>
5. Mosayebi, R., Gohari, A., Mirmohseni, M., Nasiri-Kenari, M.: Type-based sign modulation and its application for ISI mitigation in molecular communication. *IEEE Trans. Commun.* **66**(1), 180–193 (2018). <https://doi.org/10.1109/TCOMM.2017.2754492>
6. Kışlal, A.O., Pusane, A.E., Tuğcu, T.: A comparative analysis of channel coding for molecular communication. In: 2018 26th Signal Processing and Communications Applications Conference (SIU), pp. 1–4 (2018). <https://doi.org/10.1109/SIU.2018.8404368>
7. Nakano, T., Okaie, Y., Liu, J.: Channel model and capacity analysis of molecular communication with Brownian motion. *IEEE Commun. Lett.* **16**(6), 797–800 (2012). <https://doi.org/10.1109/LCOMM.2012.042312.120359>

8. Luo, Z., Lin, L., Guo, W., Wang, S., Liu, F., Yan, H.: One symbol blind synchronization in SIMO molecular communication systems. *IEEE Wirel. Commun. Lett.* **7**(4), 530–533 (2018). <https://doi.org/10.1109/LWC.2018.2793197>
9. Salehi, S., Moayedian, N.S., Javanmard, S.H., Alarcón, E.: Lifetime improvement of a multiple transmitter local drug delivery system based on diffusive molecular communication. *IEEE Trans. Nanobiosci.* **17**(3), 352–360 (2018). <https://doi.org/10.1109/TNB.2018.2850054>
10. Nakano, T., Okaie, Y., Vasilakos, A.V.: Transmission rate control for molecular communication among biological nanomachines. *IEEE J. Sel. Areas Commun.* **31**(12), 835–846 (2013)
11. Dhayabaran, B., Raja, G.T., Magarini, M., Yilmaz, H.B.: Transmit signal shaping for molecular communication. *IEEE Wirel. Commun. Lett.* **10**(7), 1459–1463 (2021). <https://doi.org/10.1109/LWC.2021.3069875>
12. Morishima, K., Fukuda, T., Arai, F., Matsuura, H., Yoshikawa, K.: Noncontact transportation of DNA molecule by dielectrophoretic force for micro DNA flow system. In: *Proceedings of IEEE International Conference on Robotics and Automation*, vol. 3, pp. 2214–2219 (1996). <https://doi.org/10.1109/ROBOT.1996.506493>
13. Zhang, T., et al.: Molecular association between diabetes-specific local gene network and nutrient metabolism modules. In: *2010 4th International Conference on Bioinformatics and Biomedical Engineering*, pp. 1–5 (2010). <https://doi.org/10.1109/ICBBE.2010.5517883>
14. Panagopoulos, D.J., Messini, N., Karabarbounis, A., Philippetis, A.L., Margaritis, L.H.: A mechanism for action of oscillating electric fields on cells. *Biochem. Biophys. Res. Commun.* **272**(3), 634–640 (2000)
15. Ming-Yan, L., Kun, S., Xu, Z., Imshik, L.: Mechanism for alternating electric fields induced-effects on cytosolic calcium. *Chin. Phys. Lett.* **26**(3), 017102 (2000)
16. Goldbeter, A., Dupont, G., Berridge, M.J.: Minimal model for signal-induced Ca^{2+} oscillations and for their frequency encoding through protein phosphorylation. *Proc. Natl. Acad. Sci. U.S.A.* **87**(4), 1461–1465 (1990)
17. Kepseu, W.D., Wofo, P.: Intercellular waves propagation in an array of cells coupled through paracrine signaling: a computer simulation study. *Phys. Rev.* **73**, 041912 (2014)